photochem

MDPI

Supporting Materials:

Metal Ion-Induced Metallogel formation by Visible-Light Responsive Phenylalanine-Functionalized Arylazopyrazole Ligands

Mikayla Browning, Alexandra Jefferson, Jazz Geter and Kesete Ghebreyessus Department of chemistry and biochemistry Hampton University, Hampton VA, 23668, USA email: Kesete.Ghebreyessus@hamptonu.edu; Tel: +1-757-727-5475

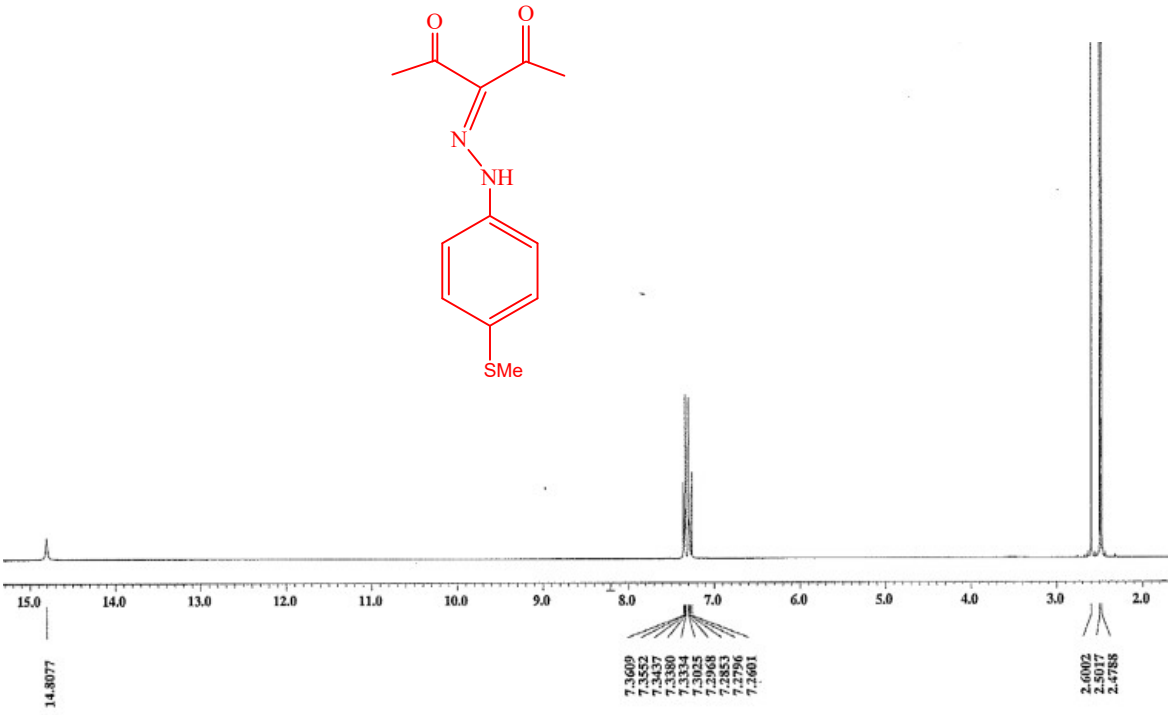

Figure S1. ^{1}H-NMR spectrum of 4-(methylthio)-3-(2-phenylhydrazono)pentane-2,4-dione (**2a**) in $CDCl_3$.

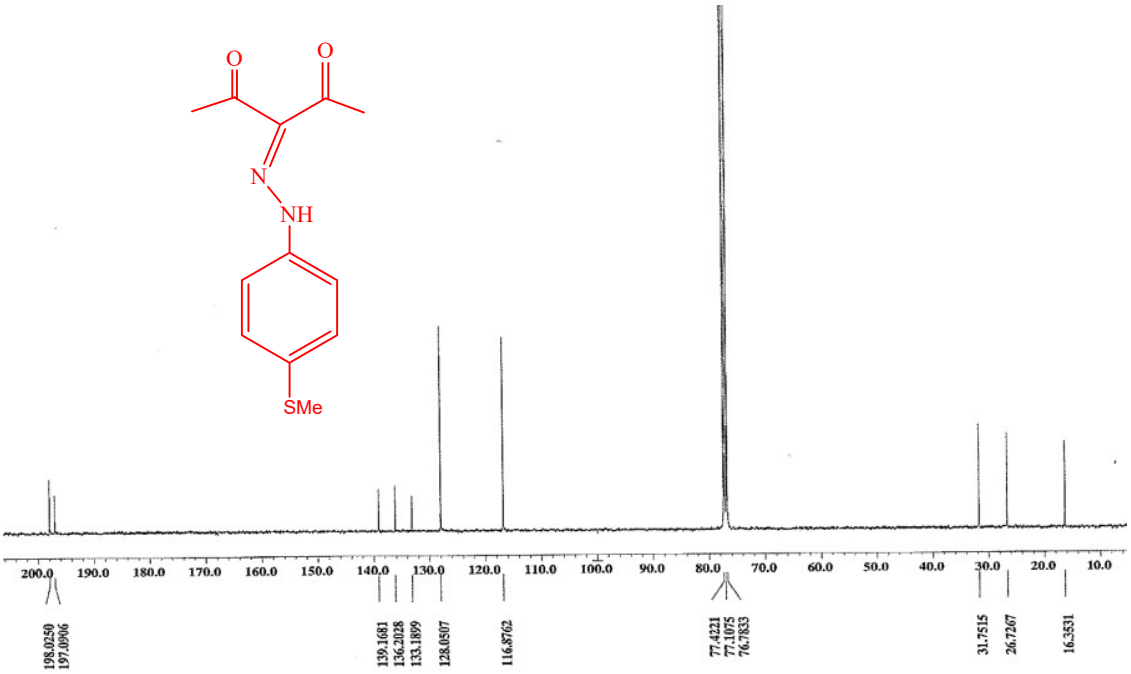

Figure S2. ^{13}C-NMR spectrum of 2-(methylthio)-3-(2-phenylhydrazono)pentane-2,4-dione (**2a**) in $CDCl_3$.

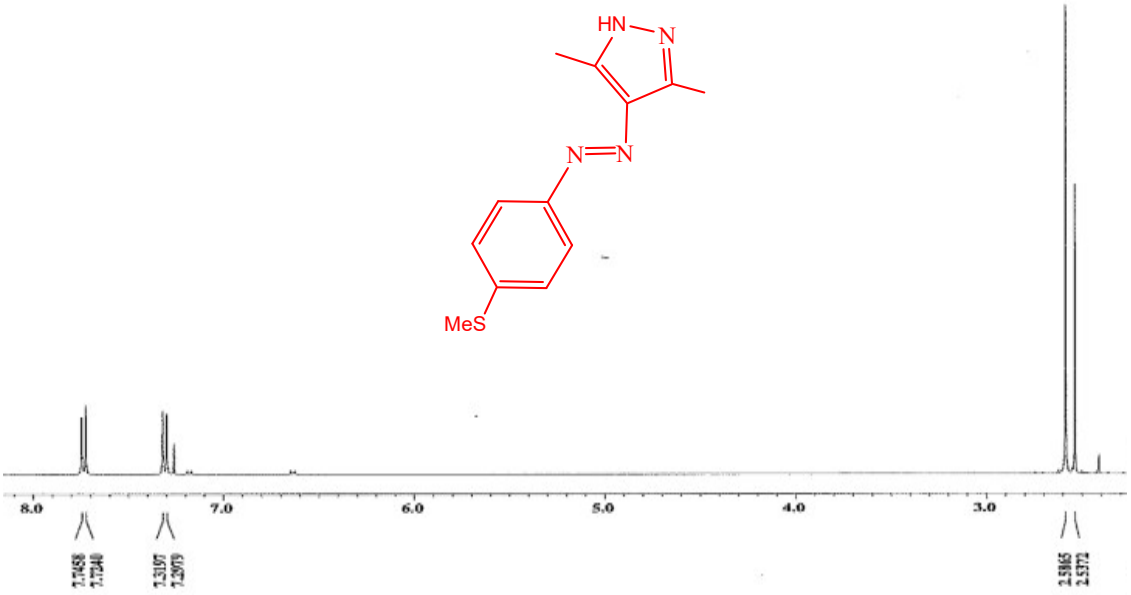

Figure S3. ^{1}H-NMR spectrum 4-(Methylthio)- 3,5-dimethyl-(4-phenyldiazenyl)-1H-pyrazole (**3a**) in $CDCl_3$.

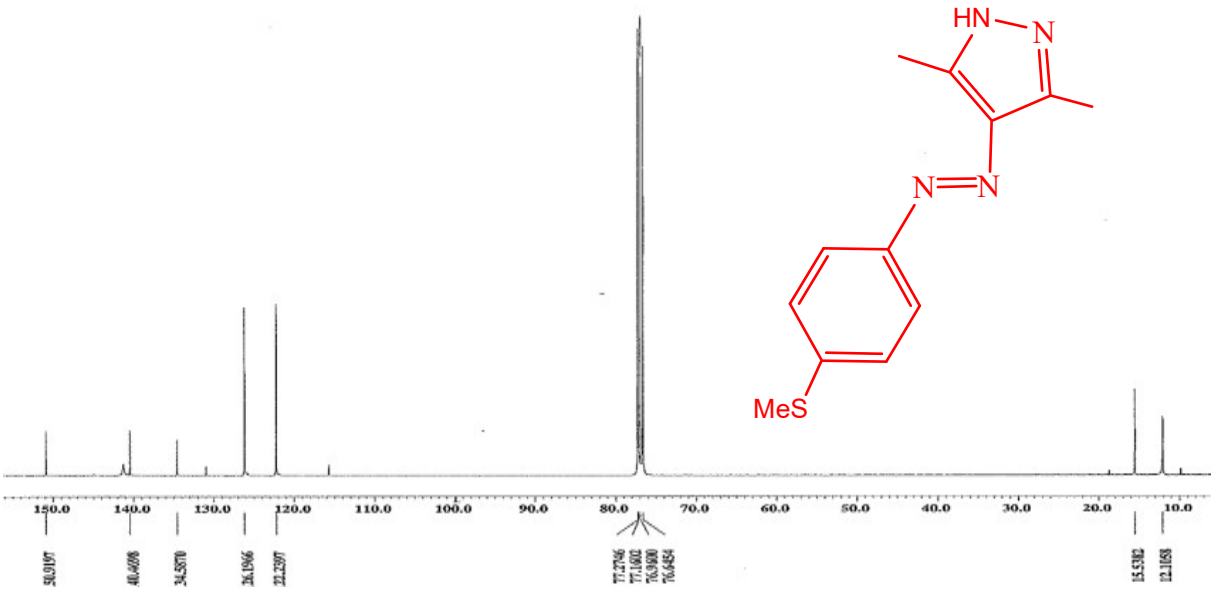

Figure S4. ^{13}C-NMR spectrum 4-(Methylthio)- 3,5-dimethyl-(4-phenyldiazenyl)-1H-pyrazole (**3a**) in $CDCl_3$.

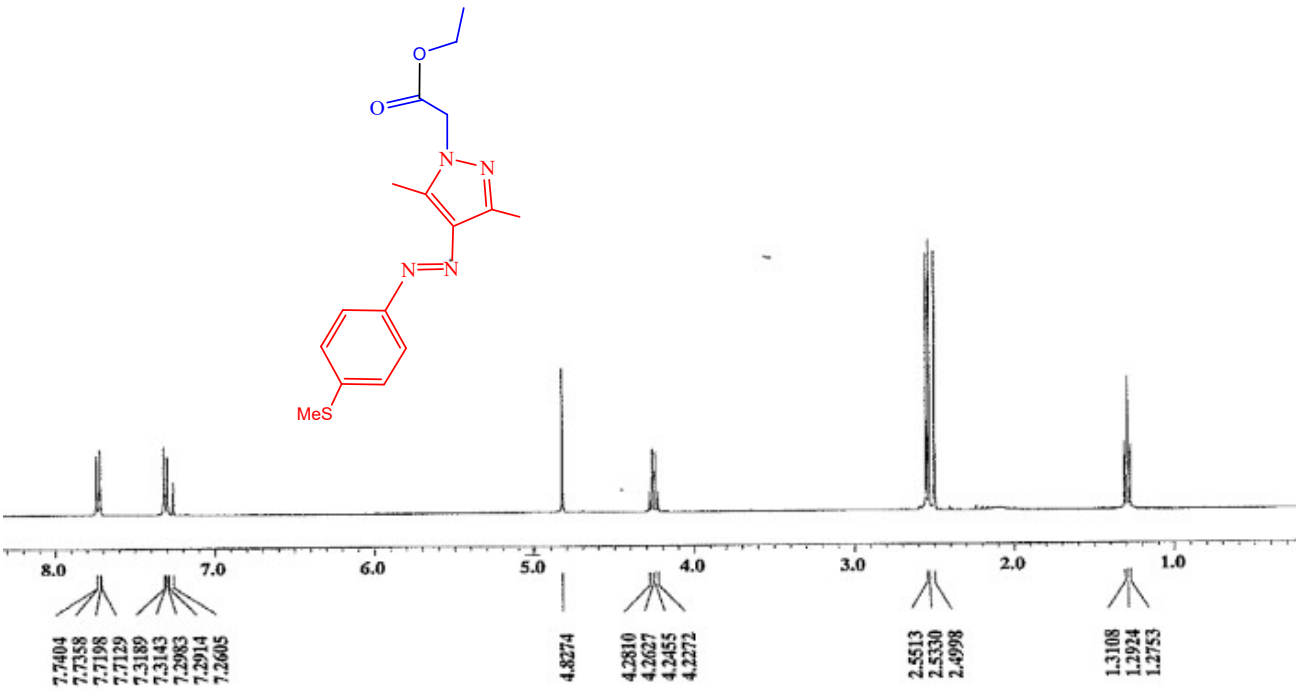

Figure S5. ^{1}H NMR spectra of 4-(Methylthio)-3,5-dimethyl-(4-phenyldiazenyl)-N-$CH_2CO_2CH_2CH_3$ **(4a)** in $CDCl_3$.

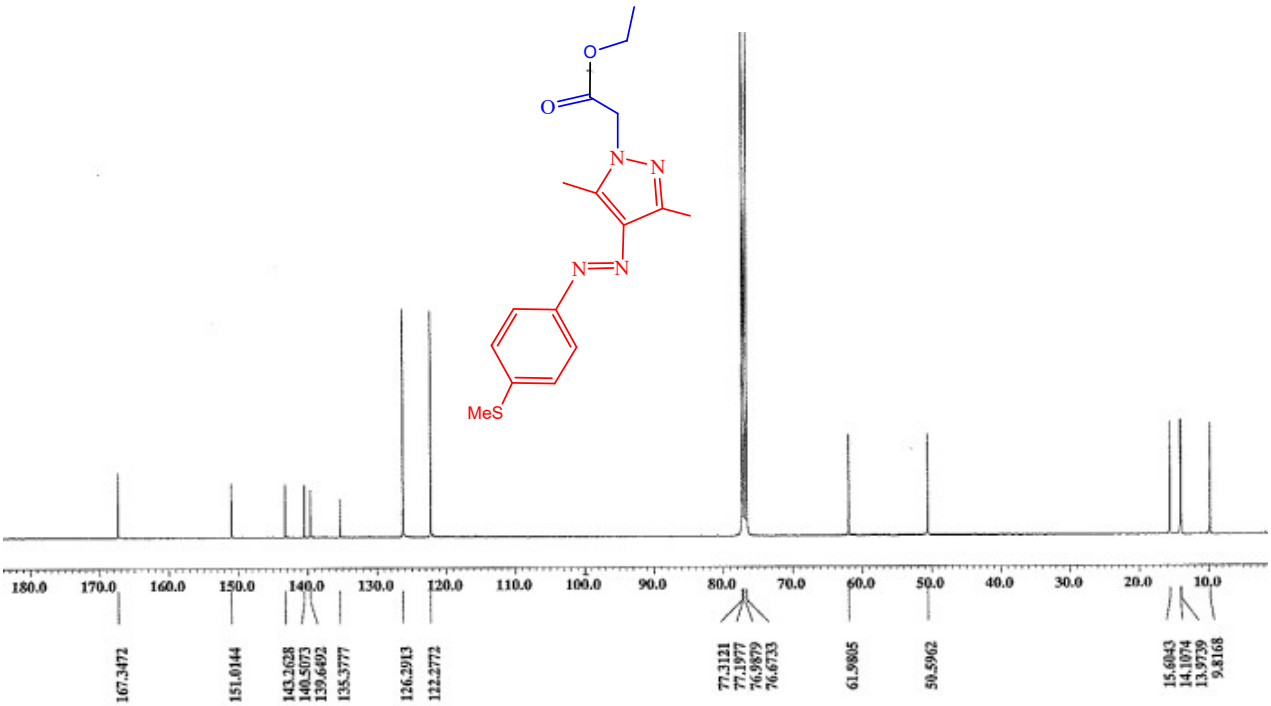

Figure S6. ^{13}C-NMR spectra of 4-(Methylthio)-3,5-dimethyl-(4-phenyldiazenyl)-N-$CH_2CO_2CH_2CH_3$ **(4a)** in $CDCl_3$.

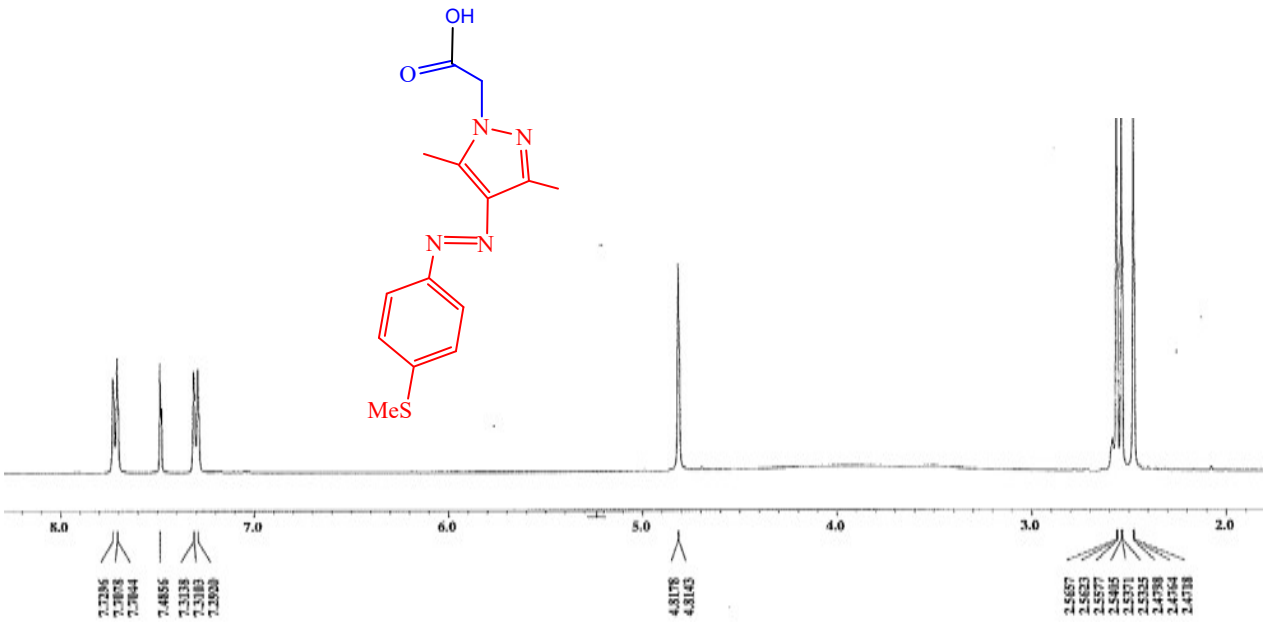

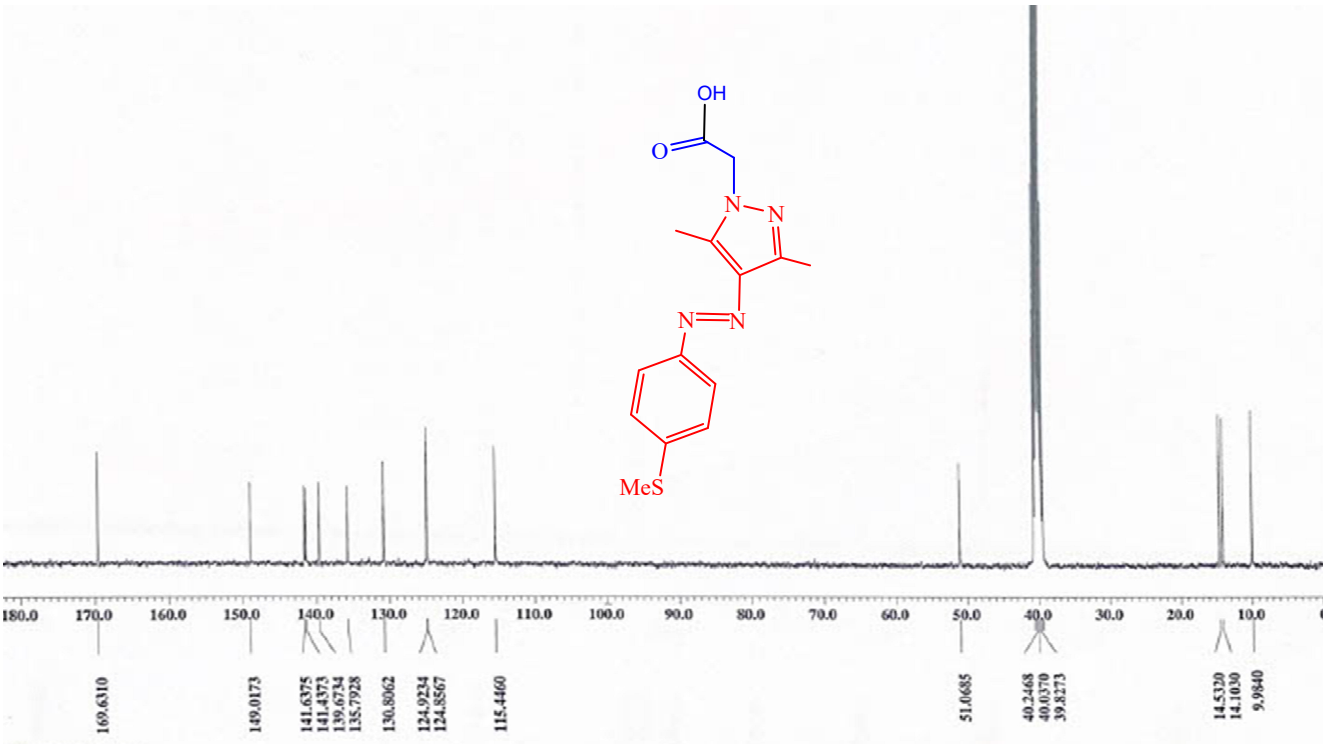

Figure S7. ^{1}H-NMR spectra for 4-(Methylthio)-3,5-dimethyl (4-phenyldiazenyl)-N-CH_2CO_2H (**5a**) in DMSO.

Figure S8. ^{13}C-NMR spectrum for 4-(Methylthio)-3,5-dimethyl (4-phenyldiazenyl)-N-CH_2CO_2H (**5a**) in DMSO.

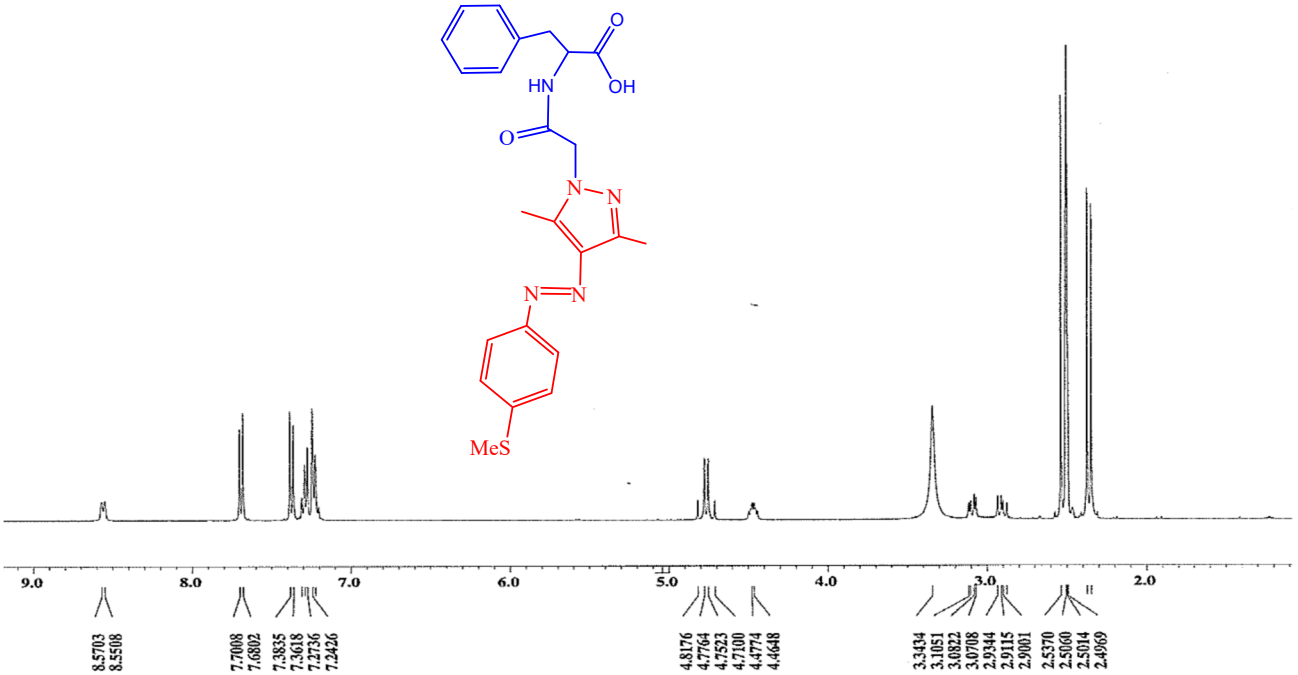

Figure S9. [1]H-NMR spectrum 4-(Methylthio)- 3,5-dimethyl-(4-phenyldiazenyl)-N-methylene-L-phenylalanine (4-MeS-AAP-NF, **6a**) in DMSO.

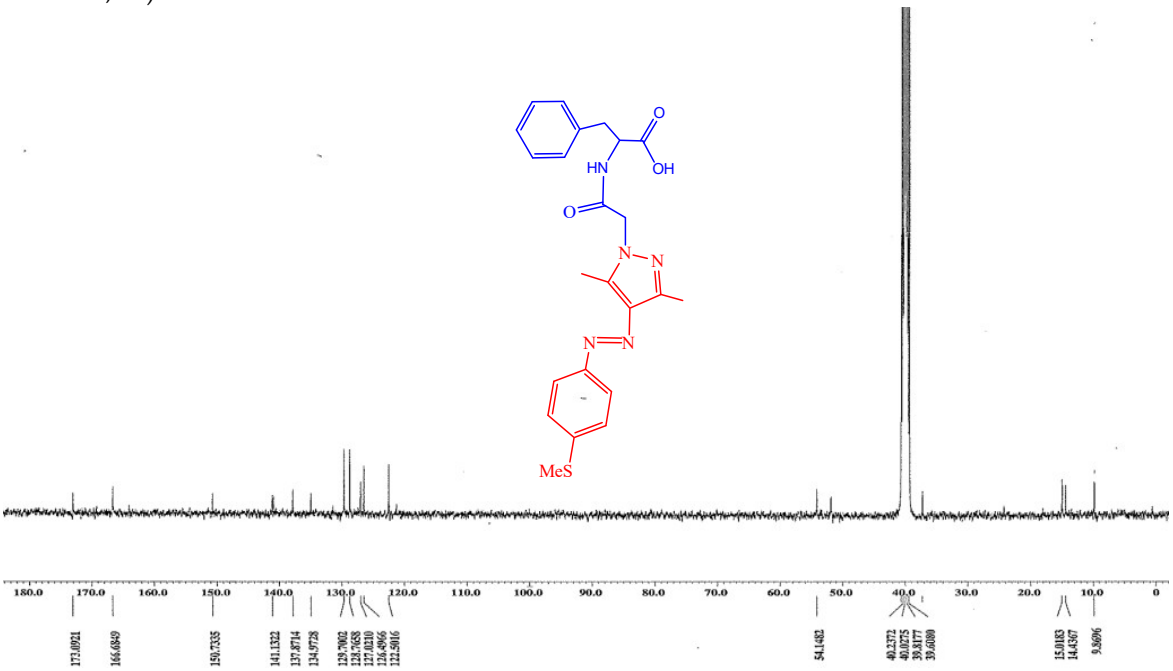

Figure S10. [13]C-NMR spectrum 4-(Methylthio)- 3,5-dimethyl-(4-phenyldiazenyl)-N-methylene-L-phenylalanine (4-MeS-AAP-NF, **6a**) in DMSO.

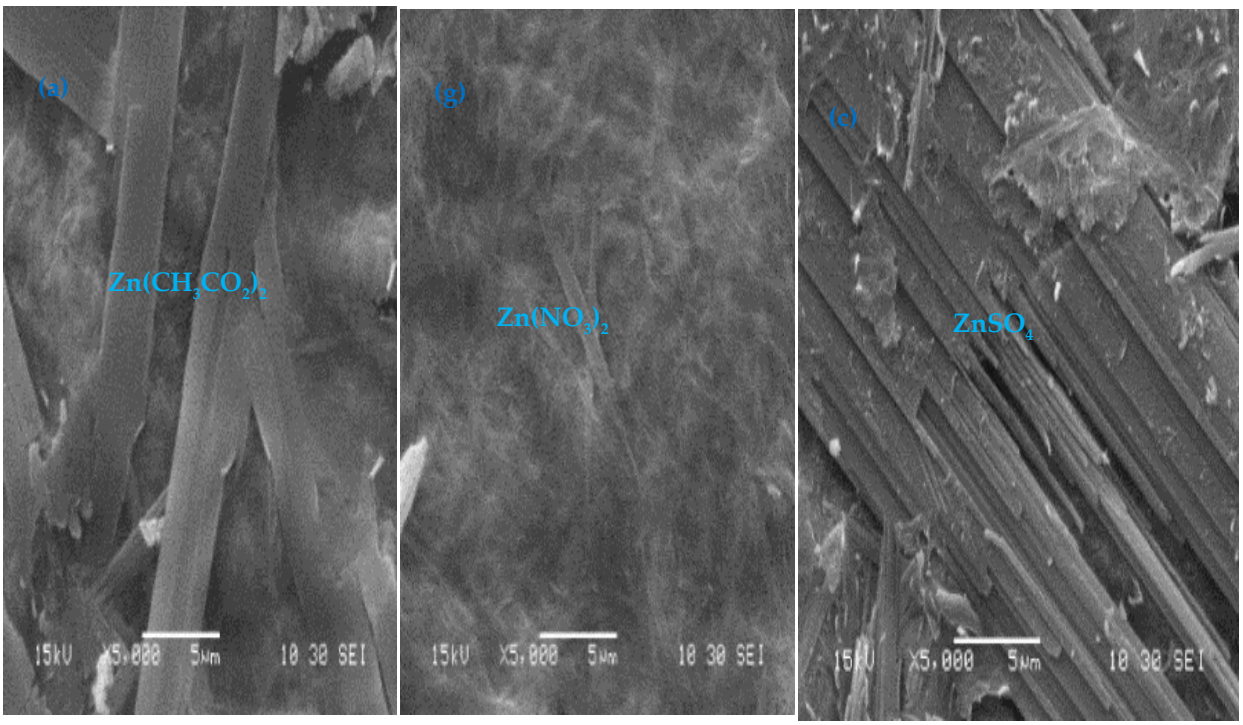

Figure S11. Dynamic strain amplitude rheological experiment for different anions of the Zn^{2+}-4-MeS-AAP-NF metallo-gels.

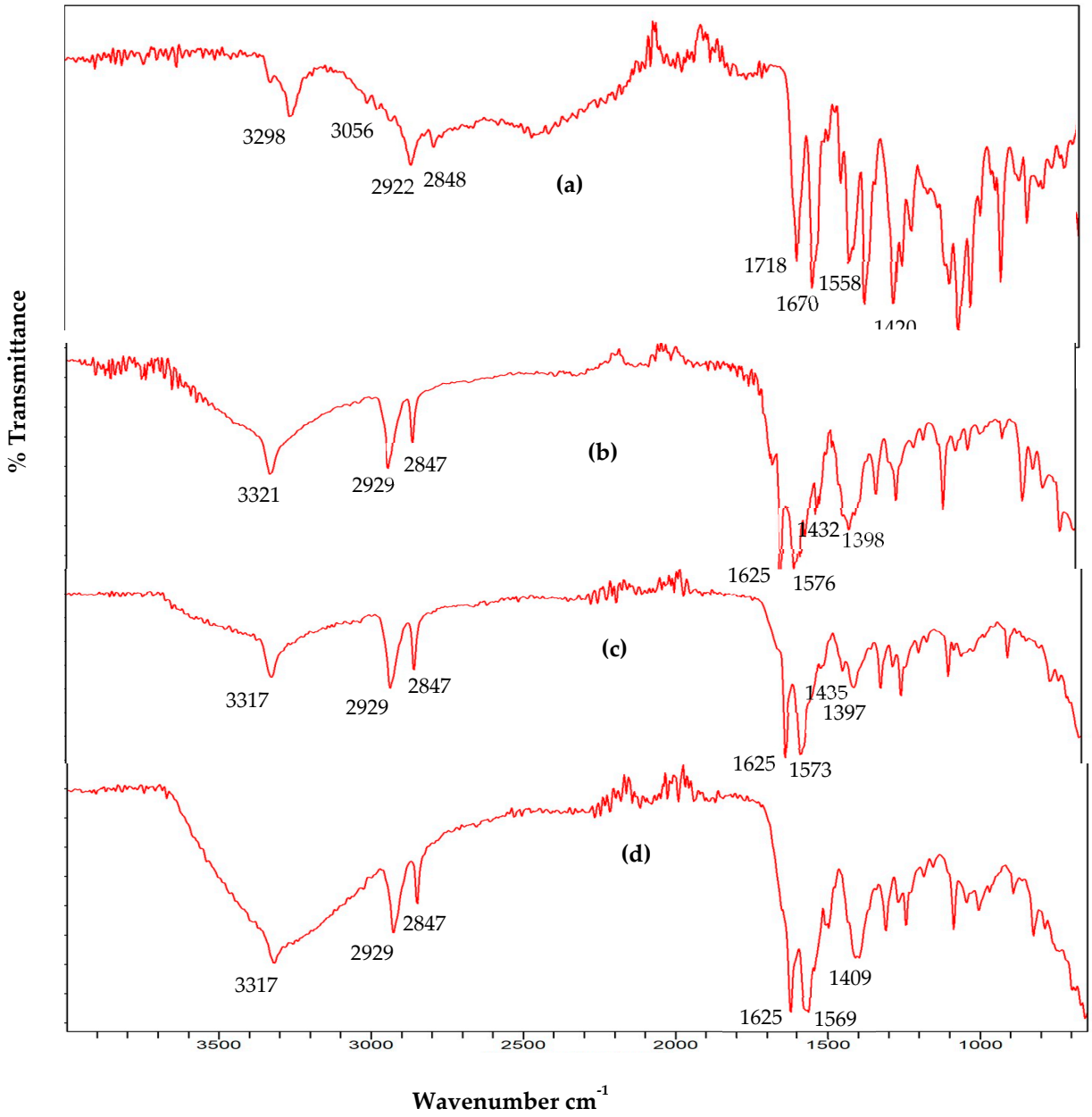

Figure S12. FTIR spectra of (a) 4-MeS-AAP-NF; (b) Cu^{2+}-4-MeS-AAP-NF; (c) Ni^{2+}-4-MeS-AAP-NF and (d) Ni^{2+}-4-MeS-AAP-NF xerogels.

$[C_{23}H_{25}N_5O_3S + H]^+$

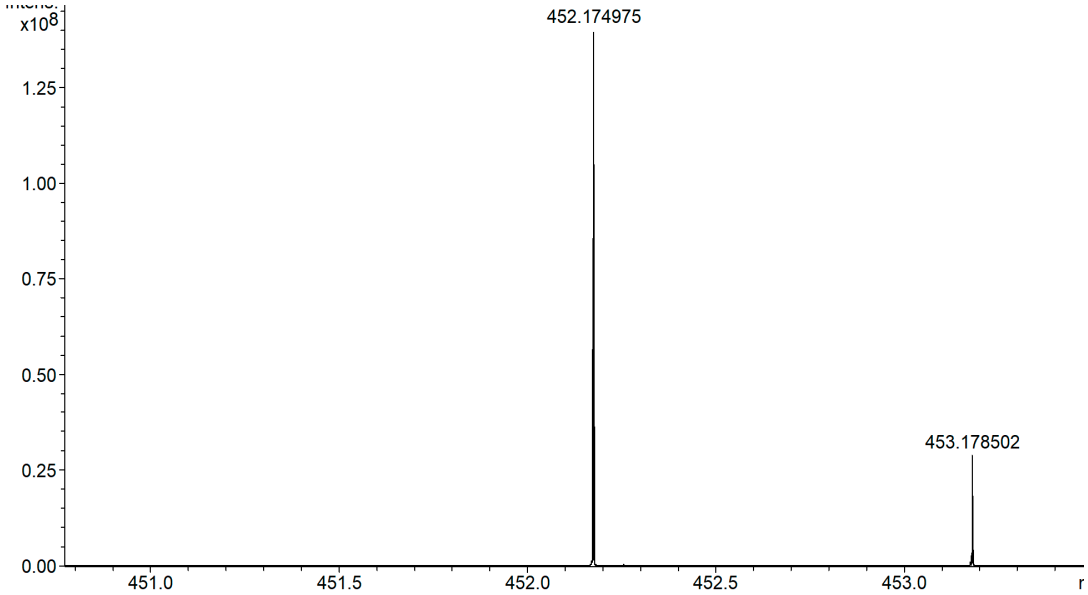

Figure S13. Electrospray ionization mass spectrum (ESI-MS) of 4-MeS-AAP-NF (**6a**).

$[C_{23}H_{24}N_5O_3S + Ca]^+$

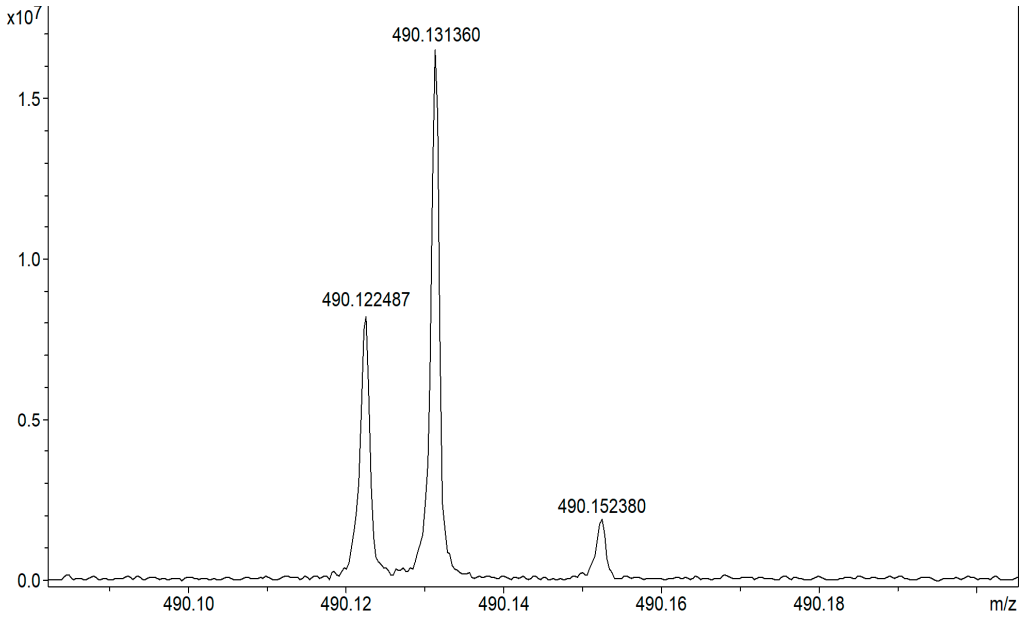

Figure S14. Electrospray ionization mass spectrum (ESI-MS) of Ca^{2+}-4-MeS-AAP-NF xerogel.

$[C_{23}H_{24}N_5O_3S + Co]^+$

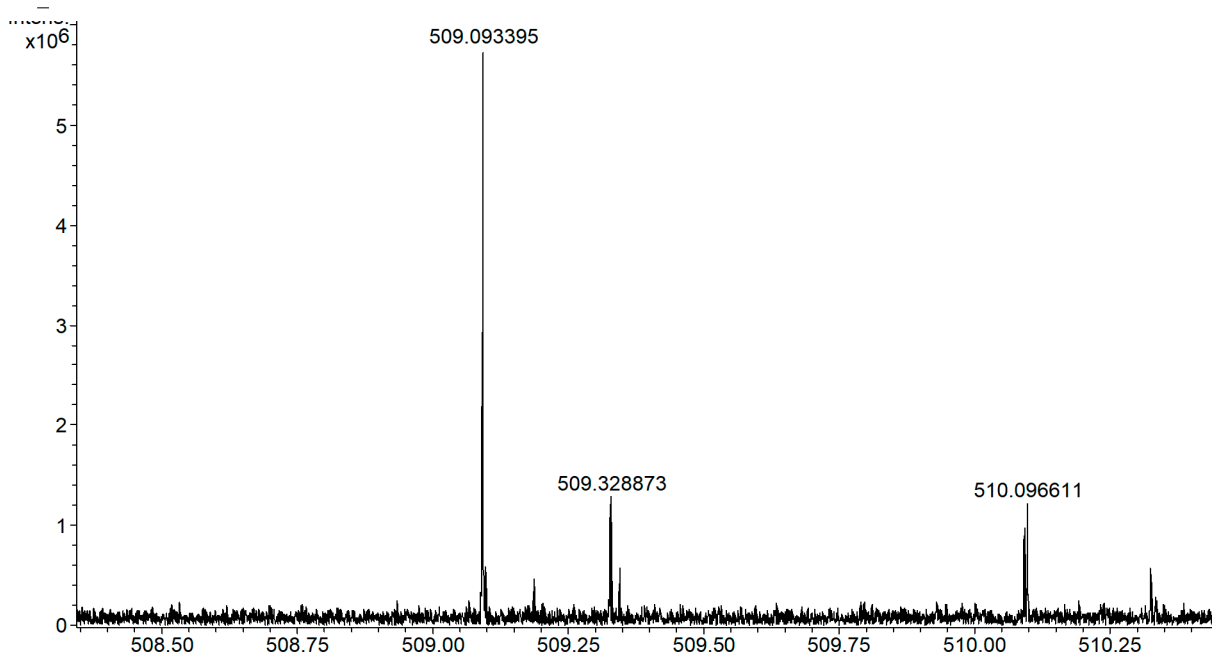

Figure S15. Electrospray ionization mass spectrum (ESI-MS) of Co^{2+}-4-MeS-AAP-NF xerogel.

$[C_{23}H_{24}N_5O_3S + Ni]^+$

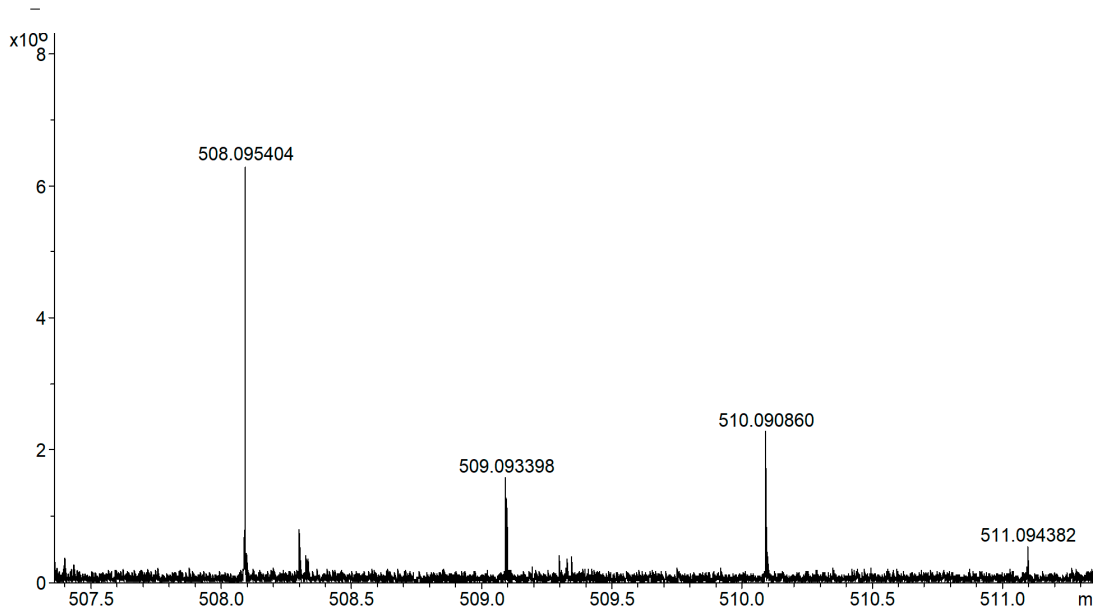

Figure S16. Electrospray ionization mass spectrum (ESI-MS) of Ni^{2+}-4-MeS-AAP-NF xerogel.

$[C_{46}H_{48}N_{10}O_6S_2 + Cu + K]^+$

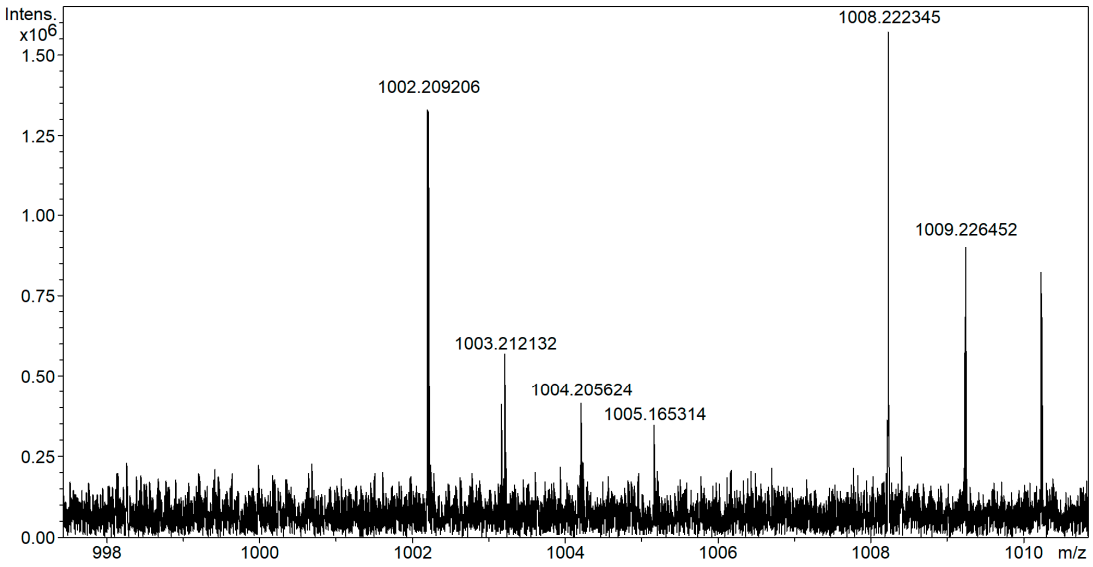

Figure S17. Electrospray ionization mass spectrum (ESI-MS) of Cu^{2+}-4-MeS-AAP-NF xerogel.